Role of Glycine 81 in (*S*)-Mandelate Dehydrogenase from *Pseudomonas putida* in Substrate Specificity and Oxidase Activity†

Asteriani R. Dewanti, Yang Xu,§ and Bharati Mitra*

Department of Biochemistry and Molecular Biology, School of Medicine, Wayne State University, Detroit, Michigan 48201

Received May 17, 2004

ABSTRACT: (*S*)-Mandelate dehydrogenase from *Pseudomonas putida* belongs to a FMN-dependent enzyme family that oxidizes (*S*)-α-hydroxyacids. Despite a high degree of sequence and structural similarity, this family can be divided into three subgroups based on the different oxidants utilized in the second oxidative half-reaction. Only the oxidases show high reactivity with molecular oxygen. Structural data indicate that the relative position of a peptide loop and the isoalloxazine ring of the FMN is slightly different in the oxidases compared to the dehydrogenases; the last residue on this loop is either an alanine or glycine. We examined the effect of the G81A, G81S, G81V, and G81D mutations in MDH on the overall reaction and especially on the suppression of activity with oxygen. G81A had a higher specificity for small substrates compared to that of wtMDH, though the affinity for (*S*)-mandelate was relatively unchanged. The rate of the first half-reaction was 20−130-fold slower for G81A and G81S; G81D and G81V had extremely low activity. Redox-potential measurements indicate that the reduction in activity is due to the decrease in electrophilicity of the FMN. The affinity for oxygen increased 10−15-fold for G81A and G81S relative to wtMDH; the rate of oxidation increased 2-fold for G81A. The increased reactivity with molecular oxygen did not correlate with the redox potentials and appears to primarily result from a higher affinity for oxygen. These results suggest that one of the ways the oxidase activity of MDH is controlled is through steric effects because of the relative positions of the FMN and the Gly81 loop.

(*S*)-Mandelate dehydrogenase (MDH)[1] from *Pseudomonas putida* oxidizes (*S*)-mandelate to benzoylformate. It is part of a metabolic pathway in Pseudomonads that allows these organisms to utilize mandelic acid, derivatized from the common soil metabolite, amygdalin, as the sole source of carbon and energy (*1*). MDH is a member of a FMN-dependent enzyme family that oxidizes (*S*)-α-hydroxyacids to α-ketoacids. The enzymes have a common reductive half-reaction in which the hydroxyacid substrate is oxidized to the ketoacid, resulting in the reduction of FMN (*2*, *3*). However, this protein family can be divided into three subgroups based on the different oxidants utilized in the second oxidative half-reaction, in which the FMN is reoxidized by electron transfer to the oxidant. The oxidases use oxygen as the final electron acceptor and produce hydrogen peroxide; in the particular case of lactate monooxygenase from *Mycobacterium smegmatis*, oxygen is first reduced to hydrogen peroxide and subsequently to water (*4*). The second subgroup consists of flavocytochrome b_2s, in which electrons are passed from the reduced flavin to an intramolecular heme cofactor in the b_2 domain and finally to an external cytochrome *c*. Membrane-bound bacterial dehydrogenases, represented by MDH, form the third subgroup; these do not have an extra cytochrome domain and most likely use an external ubiquinone as the physiological electron acceptor (*5*). MDH homologues from this subgroup are common in peripheral metabolic pathways in bacteria. One such homologue that is inducible is L-lactate dehydrogenase from *Escherichia coli*, a FMN-dependent enzyme that is induced when L-lactate is present as a food source (*6*). The reduced FMN in both the flavocytochrome b_2 and MDH subgroups has low reactivity with oxygen. Despite these differences in the second half-reaction, enzymes in the three subgroups show a high degree of sequence homology and overall three-dimensional structural similarity, as illustrated by structural studies of glycolate oxidase from spinach, flavocytochrome b_2 from *Saccharomyces cerevisiae*, and a soluble chimeric mutant of MDH, MDH-GOX2 (*7*−*10*).

Flavoproteins are known to modulate the reoxidation of reduced flavin by molecular oxygen to a great extent (*11*). Given the structural and sequence similarities in the three subgroups of the MDH family, an especially interesting question is the basis of the highly different reactivity of the reduced FMN with oxygen displayed by members of this protein family. The membrane-binding domain of MDH and presumably other membrane-bound homologues is localized to a ∼40-residue internal segment (*12*). This domain may play a role in bringing the reduced FMN in close proximity to its physiological electron acceptor in the membrane. However, it does not play a role in the discrimination against oxygen, because the soluble chimeric mutant lacking this

† This work was supported in part by an American Heart Association Postdoctoral fellowship to A.R.D.

* To whom correspondence should be addressed. Phone: (313) 577-0040. Fax: (313) 577-2765. E-mail: bmitra@med.wayne.edu.

§ Present address: Department of Pharmaceutics, University of Washington, Seattle, Washington.

[1] Abbreviations: BSA, bovine serum albumin; DCPIP, dichloroindophenol, sodium salt; $^{D}k_{cat}$, primary substrate kinetic isotope effects on k_{cat}; MDH, (*S*)-mandelate dehydrogenase; FMN_{ox}, oxidized FMN; FMN_{sq}, the semiquinone form of FMN; MDH-GOX2, a chimeric mutant of MDH with residues 177−215 replaced by residues 176−195 of glycolate oxidase from spinach.

10.1021/bi049005p CCC: $27.50
Published on Web 07/30/2004

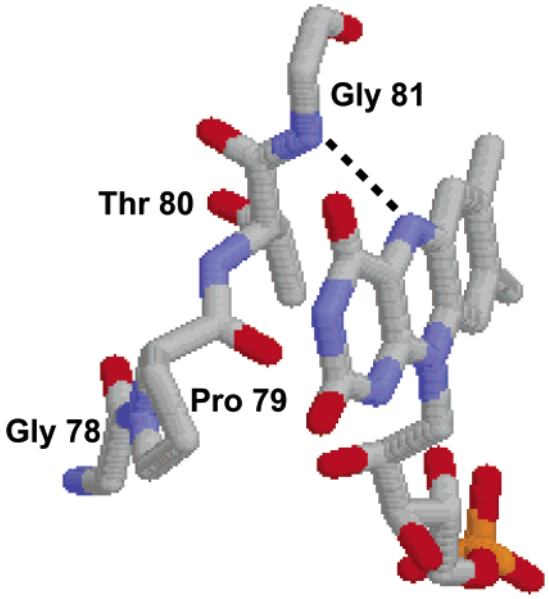

FIGURE 1: Relative positions of FMN and a four-residue loop on its *re* face in oxidized MDH-GOX2, a soluble mutant of MDH. The line represents a hydrogen bond between the N5 atom of FMN and the backbone NH of Gly81.

domain, MDH-GOX2, is also an extremely poor oxidase (*12*). In this paper, our goal was to examine the environment around the FMN in the dehydrogenase subgroups of this protein family that may prevent rapid reaction with oxygen. Reoxidation of reduced FMN by oxygen likely involves a FMN C-4a hydroperoxide intermediate (*11*). A high-resolution structure of MDH-GOX2 revealed that a glycine residue, Gly81, is in close proximity to the C-4a-N5 locus of FMN in MDH; this glycine is the last residue in a four-residue loop on the *re* face of FMN (Figure 1) (*10*). Corresponding four-residue loops are also found in a similar location in flavocytochrome b_2 and glycolate oxidase (*9*). Interestingly, a comparison of the structures of flavocytochrome b_2, glycolate oxidase, and MDH-GOX2 shows that the angle between the isoalloxazine ring of the flavin and this loop is different for glycolate oxidase relative to the two dehydrogenases (*9*−*10*). For the dehydrogenases, the isoalloxazine ring is tilted toward the loop, resulting in a hydrogen bond between the FMN N5 atom and the backbone NH of the last residue of this loop. A similar hydrogen bond is absent in glycolate oxidase; instead, there is a hydrogen bond between the FMN N5 and a water molecule that fills the void created by the FMN tilt away from the loop. Thus, it is possible that the relative positions of the FMN ring and the loop on the FMN *re* side in the three subgroups of the MDH family may play a role in controlling the reactivity with oxygen.

An alignment of the sequence of the four-residue loop in the MDH family shows that the fourth residue of the loop is either an alanine or glycine (Figure 2). Mutations of this residue have been characterized for three enzymes to date. For flavocytochrome b_2 from *S. cerevisiae*, the corresponding alanine to glycine mutation resulted in an overall decrease in activity without any change in substrate specificity; oxidase activity was not reported for the mutant (*13*). In lactate oxidase from *Aerococcus viridans*, mutation of the corresponding alanine to glycine resulted in a change in substrate specificity toward long-chain α-hydroxyacids, though the oxidase activity remained unchanged (*14*). For lactate monooxygenase, the corresponding residue is a glycine. Changing it to a larger alanine or serine resulted in a large decrease in the activity with oxygen; this was due to significant decreases in both the affinity for oxygen as well as the rate of reoxidation with oxygen. Interestingly, these mutants became true oxidases, with hydrogen peroxide as the final product instead of water (*15*−*16*). These observations indicated that this small hydrophobic residue affects the environment around FMN in important but different ways in the various subgroups of the MDH family.

In the case of the membrane-bound bacterial dehydrogenase subgroup, the last residue of the four-peptide loop is strictly a glycine residue (only a limited number of sequences is shown in Figure 2). In this study, we investigated the role of this glycine in oxidase activity as well as in the overall mechanism. Gly81 in MDH was changed to alanine, serine, valine, and aspartate, and the resulting mutants were characterized. The results reveal that Gly81 affects the rate of the first reductive reaction. More importantly, the G81A and G81S mutants show a higher oxidase activity; this primarily results from a higher affinity for oxygen. These results are discussed in relation to the structures of MDH-GOX2 in the oxidized and reduced states.

EXPERIMENTAL PROCEDURES

Materials. Oligonucleotides were purchased from Integrated DNA Technologies, Coralville, IA. Reagents were obtained from commercial sources and were of the highest possible analytical grade. 2-Hydroxyacids were from Fluka or Aldrich with the exception of 2-hydroxy-3-butynoicacid, which was from Tokyo Chemical Industry. Xanthine oxidase and horseradish peroxidase were from Sigma/Aldrich, and glucose oxidase was from Roche. For the determination of the primary substrate kinetic isotope effect, [α-^{2}H]-(*S*)-mandelic acid was enzymatically prepared as described previously (*17*).

Methods: Genetic Engineering. The mutations at Gly81 in wtMDH were generated by polymerase chain reaction methods. The oligonucleotides used for constructing the mutants G81A, G81V, G81S, and G81D had the sequences 5′-CGTTCAGTGCAGTAGGC-3′, 5′-CGTTCAGTACAGTAGGC-3′, 5′-CGTTCAGAGAAGTAGGC-3′, and 5′-CGTTCAGATCAGTAGGC-3′, respectively. The cytosolic mutant, MDH-GOX2, has been described before (*12*). The mutant MDH-GOX2/G81A was generated by restriction enzyme digestion of plasmids containing the genes encoding wtMDH/G81A and MDH-GOX2 genes, followed by ligation of the appropriate fragments. The sequences of all of the mutant genes were verified by automated DNA sequencing (DNA sequencing core facility, Wayne State University).

Enzyme Purification. For expression of histidyl-tagged wtMDH and the altered proteins, cells were typically grown at 37 °C until mid-log phase, followed by overnight induction with isopropyl β-thiogalactopyranoside at room temperature. The membrane-bound proteins were purified after extraction from membranes with detergent, according to the established protocol (*18*). The MDH-GOX2 and G81A/MDH-GOX2 proteins were cytosolic and were purified from the cytosolic portion of the cell lysate as described earlier (*12*). Protein concentrations were estimated by measuring the free FMN released upon boiling the protein solutions for 5 min.

```
                                                •
GOX       ILIDVTNIDMTTTILGFKISMPIMIAPTAMQKMAHP-EGEYATARAASA--  98
HAOX3     YLRDVSEVDTRTTIQGEEISAPICIAPTGFHCLVWP-DGEMSTARAAQA--  98
LOX       LAQDVEAPDTSTEILGHKIKAPFIMAPIAAHGLAHT-TKEAGTARAVSE-F  112

S.LDH     ILVDVRKVDISTDMLGSHVDVPFYVSATALCKLGNPLEGEKDVARGCGQGV  220
H.LDH     ILIDVKDVDISTEFFGEKTSAPFYISATALAKLGHP-EGEVAIAKGAGR--  209
Rg.MDH    VLRKMRHIDTNTTFLGIPTPLPIFVAPAGLARLGHP-DGEQNIVRGVAK--  289

Hi.LDH    VLKDMSELDTSIELFGEKLSMPTILAPVGACGMYAR-RGEVQAAQAADN--  98
Ec.LDH    ILKNMSDLSLETTLFNEKLSMPVALAPVGLCGMYAR-RGEVQAAKAADA--  98
MDH       RLVDVSRRSLQAEVLGKRQSMPLLIGPTGLNGALWP-KGDLALARAATK--  100
```

FIGURE 2: Partial sequence alignment in the region of the four-peptide loop on the *re* face of the FMN in representative members of the MDH protein family. The first three enzymes, glycolate oxidase from spinach (GOX) (*31*), human peroxisomal oxidase (HAOX3) (*32*), and lactate oxidase from *A. viridans* (LOX) (*33*), belong to the oxidase subgroup. The flavocytochrome b_2 subgroup is represented by lactate dehydrogenase from *S. cerevisiae* (S.LDH) (*34*), lactate dehydrogenase from *Hansenula anomala* (H.LDH) (*35*), and mandelate dehydrogenase from *Rhodotorula graminis* (Rg.MDH) (*36*). The third subgroup represents bacterial membrane-bound dehydrogenases, a putative lactate dehydrogenase from *Haemophilus influenza* (Hi.LDH) (Genebank accession number 3212238), lactate dehydrogenase from *E. coli* (Ec.LDH) (*6*) and mandelate dehydrogenase from *P. putida* (MDH) (*1*).

Steady-State and Presteady-State Kinetics of the Reductive Half-Reaction. Steady-state dehydrogenase activities were typically measured in 0.1 M potassium phosphate buffer at pH 7.5, containing 1 mg/mL bovine serum albumin (BSA), 1 mM phenazine methosulfate, and 100−150 μM dichlorindophenol (DCPIP), at 20 °C, as described previously for wtMDH (*18*). Substrate kinetic isotope effects were measured using [α-^{2}H]-(*S*)-mandelate. Stopped-flow data for the FMN reductive reaction were collected at 20 °C in 0.1 M potassium phosphate at pH 7.5 under anaerobic conditions. Solutions were made anaerobic by saturating them with argon. The reduction of FMN was monitored by following the decrease in absorbance at 460 nm after the addition of different concentrations of (*S*)-mandelate. The stopped-flow data were adequately described by a single-exponential fit, unless noted otherwise.

Steady-State and Presteady-State Measurements of the Oxidase Activity. The formation of H_2O_2 was measured in the steady state using a coupled-enzyme assay, using horseradish peroxidase and *o*-dianisidine. The assay mixture contained 0.1 M phosphate buffer at pH 7.5, 14 μg/mL horseradish peroxidase, 0.27 mg/mL *o*-dianisidine (dissolved in 20% Triton X-100), and (*S*)-mandelate. Formation of the *o*-dianisidine radical cation, which reflects the oxidase activity of the enzyme, was monitored at 460 nm and at 20 °C ($\epsilon = 11.3$ mM^{-1} cm^{-1} at 460 nm). To generate different concentrations of oxygen in the assay mix, the buffer was saturated with a gaseous mixture containing different ratios of nitrogen and oxygen. After the addition of horseradish peroxidase and (*S*)-mandelate, the assay mix was again saturated with the desired concentration of oxygen gas for a further 10 min, before starting the reaction with the addition of protein.

The reoxidation of reduced wtMDH, G81A, or G81S with oxygen was measured in the stopped-flow spectrophotometer at 20 °C as follows. One syringe was filled with the enzyme reduced with 5−50-fold excess of (*S*)-mandelate under anaerobic conditions in 0.1 M potassium phosphate at pH 7.5. The second syringe was filled with a buffer saturated with different concentrations of oxygen and the same concentration of (*S*)-mandelate as in the first syringe.

Measurement of Redox Potentials. Redox potentials of wtMDH and the mutant proteins were measured using indicator dyes according to established procedures (*19*). A total of 10 μM enzyme in 0.1 M potassium phosphate at pH 7.5, ~7 μM indigo disulfonate ($E_m = -0.125$ V), 500 μM xanthine, and ~8 μM benzyl viologen (to ensure rapid equilibration of reducing equivalents) were added to a cuvette fitted with a sidearm. A total of 0.3 μL of 20 units/mL xanthine oxidase was added to the sidearm. The solutions were saturated with argon for 1 h. After anaerobic conditions were established, the starting spectrum of the solution was recorded. The reductive reaction was then started by adding xanthine oxidase from the sidearm. The data were collected over 3−4 h to ensure that equilibrium was maintained at all time. To establish that the method was accurately followed, the redox potential of glucose oxidase was measured using the same procedure at two different pHs, 5.3 and 9.3, and compared to reported values. Redox potential values obtained for glucose oxidase were −83 and −215 mV at pH 5.3 and 9.3, respectively, in good agreement with values reported in the literature (*20*).

Binding of Sulfite. The binding of sulfite to the mutant enzymes was measured at 4 °C in 20 mM phosphate buffer at pH 7.5, containing 10% ethylene glycol. The dissociation constants were obtained from spectral titration of the oxidized enzymes (20 μM) as described previously (*12*).

Instrumentation. UV−visible spectra were recorded with a Varian (Cary 1E) spectrophotometer. Stopped-flow data were collected using an Applied Photophysics System SX 18.MV spectrophotometer equipped with a diode-array accessory.

RESULTS

Purification and Properties of the Gly81 Mutants. The level of protein expression was checked by Western blotting using an antibody against the hexahistidyl tag. The levels of expression of the membrane-bound Gly81 mutants were similar to that of wtMDH, with the exception of G81S, which was slightly lower. Expression of the cytosolic MDH-GOX2 and MDH-GOX2/G81A were similar to that of G81S. The yields of purified protein per gram of cell paste followed a similar pattern; the yield for G81S, MDH-GOX2, and G81A/MDH-GOX2 was half that of wtMDH and the other Gly81 mutants.

Figure 3 shows the absorbance spectra of the Gly81 mutant enzymes together with wtMDH and MDH-GOX2. Both

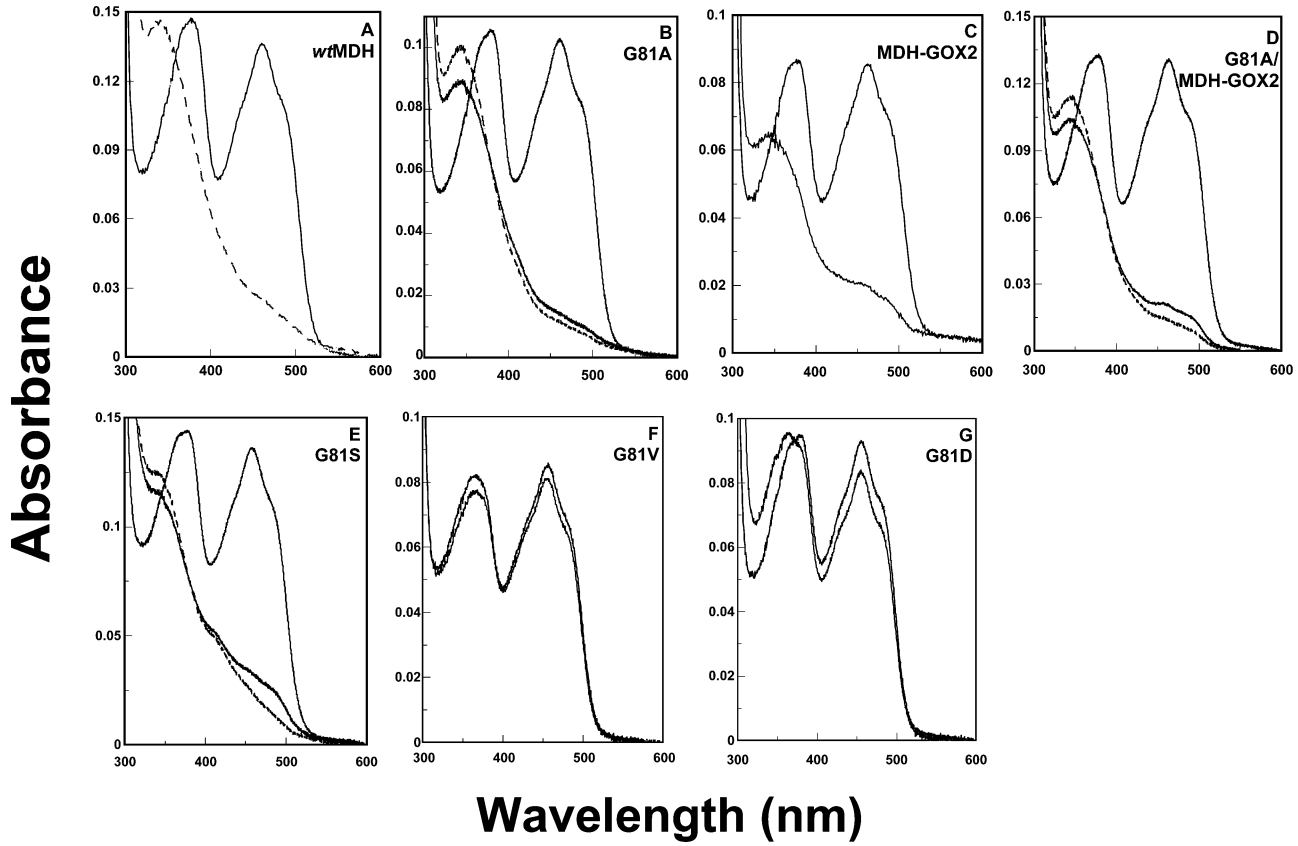

FIGURE 3: Absorbance spectra of the Gly81 mutants in 20 mM potassium phosphate at pH 7.5, with 10% ethylene glycol and 0.1% Tween 80 under aerobic conditions. (A) wtMDH, (B) 8.2 μM G81A, (C) 6.9 μM MDH-GOX2, (D) 9.7 μM G81A/MDH-GOX2, (E) 10.9 μM G81S, (F) 7.3 μM G81V, and (G) 8.3 μM G81D. For each panel, the spectrum of the oxidized protein is a black solid line, the spectrum of the enzyme reduced with ~8 mM (*S*)-mandelate under aerobic conditions is a gray solid line, and the spectrum of the reduced enzyme under anaerobic conditions is a black dashed line.

Table 1: Kinetic Parameters (Steady and Presteady States) of the Gly81 Mutants at 20 °C[a]

	k_{cat} (s^{-1})	K_m (mM)	k_{red} (s^{-1})	K_d (mM)	$^{D}k_{cat}$
wtMDH	360 ± 8	0.13 ± 0.01	402 ± 16	0.19 ± 0.03	2.1
G81A	19.2 ± 0.4	0.15 ± 0.01	17.4 ± 0.7	0.33 ± 0.06	5.4
G81S	2.8 ± 0.1	2.3 ± 0.2	2.6 ± 0.1	4.1 ± 0.3	5.5
G81D	0.11 ± 0.004	2.0 ± 0.2	nd[b]	nd	nd
G81V	0.050 ± 0.004	0.17 ± 0.06	nd	nd	nd
MDH-GOX2	205 ± 4	0.09 ± 0.01	771 ± 37[c]	0.23 ± 0.3[c]	2.6
G81A/MDH-GOX2	2.3 ± 0.07	0.04 ± 0.005	1.8 ± 0.03	0.02 ± 0.002	5.2

[a] Steady-state and presteady-state assays, using (*S*)-mandelate as the substrate, were performed in 0.1 M potassium phosphate at pH 7.5. For steady-state assays, 100−150 μM DCPIP, 1 mg/mL BSA, and 1 mM phenazine methosulfate were also included. $^{D}k_{cat}$ = primary substrate kinetic isotope effect on k_{cat}. [b] nd = not determined. [c] As noted in the Results, these parameters were obtained for the initial fast phase of the reaction, for which no substrate inhibition was observed.

oxidized wtMDH and MDH-GOX2 have absorbance peaks at 378 and 460 nm. G81A, G81S, and MDH-GOX2/G81A have similar FMN spectra compared to wtMDH and MDH-GOX2. However, for G81D and G81V, the absorbance peak at 460 nm is blue-shifted to 456 and 455 nm, respectively; additionally, for G81V, the peak at 378 nm is shifted to 365 nm. These changes in the absorbance spectra suggest that the environment around FMN is somewhat perturbed when Gly81 is replaced by a larger, hydrophobic residue or by a negatively charged residue. When (*S*)-mandelate was added under anaerobic conditions, all of the proteins were completely reduced with the exception of G81D and G81V. As shown below, these two mutants have extremely low activities; it is probable that the FMN in these mutants is in an orientation such that substrate oxidation and flavin reduction are not favorable.

Kinetic Parameters. The steady-state and presteady-state kinetic parameters for wtMDH and the G81 mutants are listed in Table 1. The k_{cat} values for G81A and G81S are similar to the k_{red} values, implying that they are similar to wtMDH; the rate-limiting step in catalysis occurs in the first reductive half-reaction. G81A has ~20-fold lower k_{cat} and k_{red} values relative to wtMDH, while the K_d for the substrate is ~2-fold higher. The activity of G81S is much lower; its k_{cat} and k_{red} values are ~150-fold lower, while the affinity for (*S*)-mandelate is 20-fold weaker. The G81D and G81V mutants have extremely low activities, in accordance with our earlier observation that the FMN in these mutants could not be reduced fully by (*S*)-mandelate.

The cytosolic chimeric mutant, MDH-GOX2, is highly active and has steady-state parameters that are similar to those of the membrane-bound wtMDH (Table 1) (*10*). However,

Table 2: Comparison of Substrate Specificity of wtMDH and G81A[a]

	wtMDH			G81A		
substrate	k_{cat} (s^{-1})	K_m (mM)	k_{cat}/K_m (s^{-1} mM^{-1})	k_{cat} (s^{-1})	K_m (mM)	k_{cat}/K_m (s^{-1} mM^{-1})
(*S*)-mandelate	360 ± 8	0.13 ± 0.01	2769	19.2 ± 0.4	0.15 ± 0.01	128
mandelate	350 ± 10	0.24 ± 0.02	1458	15.2 ± 0.3	0.24 ± 0.02	63.3
4-chloromandelate	334 ± 6	0.27 ± 0.04	1237	9.3 ± 0.3	0.43 ± 0.04	21.6
indoleglycolate	122 ± 14	0.40 ± 0.03	305	1.2 ± 0.03	0.63 ± 0.05	1.9
3-phenyllactate	0.52 ± 0.01	2.0 ± 0.1	0.26	0.15 ± 0.002	0.37 ± 0.02	0.4
3-indolelactate	1.0 ± 0.01	0.9 ± 0.1	1.1	0.27 ± 0.01	0.17 ± 0.01	1.6
2-hydroxyoctanoate	0.5 ± 0.06	0.8 ± 0.1	0.63	0.26 ± 0.01	0.14 ± 0.01	1.9
2-hydroxyisocaproate	0.8 ± 0.05	4.3 ± 0.2	0.19	0.48 ± 0.02	1.6 ± 0.1	0.3
2-hydroxyhexanoate	0.34 ± 0.02	4.9 ± 0.4	0.07	0.19 ± 0.008	1.4 ± 0.2	0.14
2-hydroxyvalerate	0.36 ± 0.01	15.3 ± 1.5	0.024	0.27 ± 0.02	6.4 ± 1.0	0.04
2-hydroxybutyrate	0.10 ± 0.01	32.0 ± 3.5	0.003	0.37 ± 0.03	4.4 ± 1.0	0.08
2-hydroxy-3-butynoate	3.9 ± 0.1	22.0 ± 1.5	0.177	14.8 ±0.6	4.3 ± 0.5	3.4

[a] Unless specified, all of the substrates are racemic mixtures. Steady-state assays were performed at 20 °C as described in Table 1.

unlike wtMDH, we observed biphasic kinetics during presteady-state measurements for MDH-GOX2. The first phase was fast, about 3−4-fold faster than the steady-state rate. The slower phase was strongly inhibited by substrate concentrations above 50 μM. Substrate inhibition was not observed in either the steady-state or the fast, initial phase of the reaction for MDH-GOX2. The reason for this inhibition is unknown. Substrate inhibition has not been observed for wtMDH in either the steady-state or the presteady-state.

The G81A mutation in MDH-GOX2, G81A/MDH-GOX2, has a 100-fold lower k_{cat} relative to MDH-GOX2 itself but a higher affinity for the substrate, unlike the case with wtMDH and the G81A pair. The k_{cat}/K_m parameter is 20-fold lower for G81A relative to wtMDH and 40-fold lower for G81A/MDH-GOX2 relative to MDH-GOX2. In other words, introducing the alanine mutation at residue 81 results in a similar decrease of the specificity constant for (*S*)-mandelate for both the membrane-bound wtMDH and the cytosolic MDH-GOX2, though it is slightly more deleterious for the latter.

Both wtMDH and MDH-GOX2 have a relatively low substrate kinetic isotope effect ($^{D}k_{cat}$) of about 2.1−2.6. In contrast, the G81A, G81S, and G81A/MDH-GOX2 mutants all had a much higher $^{D}k_{cat}$ of 5.2−5.5.

We have previously reported that for wtMDH, a transient intermediate is observed during the reductive reaction at low temperature (*21*). This is a charge-transfer complex of oxidized FMN with an electronegative intermediate. When the reductive reaction of G81A was monitored at 4 °C, a similar intermediate was observed. Its maximal extinction coefficient (at 560 nm) was extremely low, precluding a detailed kinetic analysis. However, it was evident that both its rate of formation and rate of disappearance were significantly slowed relative to that of wtMDH.

Substrate Specificity of wtMDH and G81A. Because the introduction of alanine in place of Gly81 resulted in a decrease of the k_{cat}/K_m parameter for (*S*)-mandelate, we next examined the effect of this substitution on other substrates. A comparison of the steady-state kinetic parameters of wtMDH and G81A is shown in Table 2. wtMDH is highly specific toward its physiological substrate, (*S*)-mandelate. The specificity decreases rapidly with both the decrease in the size of the substrate side chain as well as loss of unsaturation at the β carbon of the substrate (*18*). G81A follows the same pattern as wtMDH, in preferring substrates with unsaturation at the β carbon. However, unlike the case with (*S*)-mandelate, similar k_{cat} values are obtained for G81A and wtMDH when using substrates with smaller side chains; additionally, the K_m values for the smaller substrates are in fact, lower for G81A relative to wtMDH. In particular, G81A had higher k_{cat} and k_{cat}/K_m values than wtMDH for the 4-carbon substrates, 2-hydroxybutyrate and 2-hydroxy-3-butynoate; G81A is a significantly better enzyme relative to wtMDH when using 2-hydroxy-3-butynoate as the substrate. A similar observation was made when comparing MDH-GOX2 with G81A/MDH-GOX2; the specificity toward smaller substrates improved for G81A/MDH-GOX2 relative to MDH-GOX2 (data not shown).

Reactivity Toward Oxygen. In the absence of any other electron acceptor, oxygen is used by wtMDH for reoxidation of the reduced flavin, though at a rather slow rate. When both (*S*)-mandelate and oxygen concentrations were varied in the steady-state reaction, the data fit to a parallel-line pattern in double-reciprocal plots (data not shown). This implies that when oxygen is used as the second substrate in our assays, the enzyme follows ping-pong kinetics. A similar observation was made earlier when using the dye DCPIP as the second substrate (*18*). Table 3 shows the kinetic parameters obtained with oxygen as the oxidant. The steady-state parameters, $k_{cat}(O_2)$ and $K_m(O_2)$, have fairly large errors associated with them, a result of overall low activities and using a coupled enzyme assay system. Nevertheless, it is evident that G81A has a higher activity with oxygen relative to wtMDH. The $k_{cat}/K_m(O_2)$ parameter is ∼8-fold higher for G81A relative to wtMDH. G81S has a similar value as wtMDH. G81D and G81V have extremely low activities with oxygen. G81V appears to have an unusually low K_m for oxygen; however, given the very low activities and the large errors, the results with G81V and G81D are not conclusive. The soluble MDH-GOX2 has a surprisingly low activity with oxygen relative to wtMDH. However, G81A/MDH-GOX2 has a 10-fold higher $k_{cat}/K_m(O_2)$ relative to MDH-GOX2. Therefore, introducing the G81A mutation in wtMDH and in MDH-GOX2, results in a similar increase in activity with oxygen, though the overall rates with the soluble proteins are rather low.

Given the large errors associated with measuring hydrogen peroxide formation, we wanted to ensure that the trends we observed were real by measuring the rate of reoxidation of

Table 3: wtMDH and the Gly81 Mutants: Activities with Oxygen as the Electron Acceptor and Redox Potentials[a]

	k_{cat} (s^{-1})	$K_m(O_2)$ (mM)	k_{ox} (s^{-1})	$K_d(O_2)$ (mM)	redox potential[b] ox/sq (mV)
wtMDH	1.2 ± 0.7	3.2 ± 1.9	2.5 ± 0.9	2.3 ± 0.9	−91 ± 4
G81A	3.4 ± 0.7	1.1 ± 0.25	5.3 ± 0.3	0.21 ± 0.02	−118 ±10
G81S	0.61 ± 0.45	1.4 ± 1.0	1.35 ± 0.06	0.16 ± 0.01	−112 ± 6
G81D	0.05 ± 0.03	0.22 ± 0.18	nd[c]	nd	−121 ± 10
G81V	0.07 ± 0.00	0.04 ± 0.01	nd	nd	−107 ± 9
MDH-GOX2	0.03 ± 0.01	0.68 ± 0.28	nd	nd	−91 ± 2
G81A/MDH-GOX2	0.22 ± 0.04	0.49 ± 0.07	nd	nd	−121 ± 14

[a] Steady-state and presteady-state assays were performed at 20 °C as described in Table 1. For the presteady-state k_{ox} values, the enzymes were reduced anerobically with 5-fold excess (*S*)-mandelate for wtMDH and G81A and 50-fold excess (*S*)-mandelate for G81S, before initiating the reoxidation with oxygenated buffer. [b] Redox potentials were measured in 0.1 M potassium phosphate at pH 7.5 for the soluble mutants and in 20 mM potassium phosphate at pH 7.5, 0.1% Tween-80, and 10% ethylene glycol for the membrane-bound proteins. [c] nd = not determined.

reduced FMN with oxygen directly in the stopped-flow spectrophotometer. Because wtMDH and G81A have relatively low K_m values with (*S*)-mandelate (Table 1), they were reduced with 5-fold excess substrate. G81S could only be fully reduced with a 50-fold excess substrate. Reoxidation of the reduced enzymes was followed using buffer equilibrated with different concentrations of oxygen. The k_{ox} and $K_d(O_2)$ parameters were consistently more reproducible and had more reasonable errors associated with them. The $k_{ox}/K_d(O_2)$ parameter is ~23-fold higher for G81A and ~8-fold higher for G81S, relative to that for wtMDH. The major difference between the two mutants and wtMDH was the substantially increased affinity for oxygen, such that the $K_d(O_2)$ values for the mutants were lower than the atmospheric oxygen concentration (0.27 mM). Because of the low activities and high K_m values for (*S*)-mandelate obtained with the other Gly81 mutants (Table 1), we did not attempt stopped-flow measurements of the oxidative reaction for G81D and G81V.

The similarity of the steady-state rates of hydrogen peroxide formation and the rate of reoxidation of reduced wtMDH by oxygen in stopped-flow experiments for wtMDH, G81A, and G81S indicates that hydrogen peroxide is the primary product of reducing oxygen and not water.

Inhibition by Sulfite. Sulfite inhibits α-hydroxyacid-oxidizing enzymes by forming a tight covalent adduct with oxidized FMN. The strength of the adduct reflects the environment around FMN. The dissociation constants for the adducts with G81A, G81S, and G81D were measured by titration with increasing amounts of sulfite at 4 °C and pH 7.5, as described earlier (*18*). K_d values obtained for G81A and G81S were 22 ± 3.2 and 2.6 ± 0.2 μM, respectively. The K_d for the adduct with wtMDH is 30 μM (*18*). Not surprisingly, sulfite did not appear to bind to G81D at all. These results indicate that the FMN environment in G81A is relatively unchanged relative to that in wtMDH. The higher affinity of sulfite for FMN in G81S probably results from an additional interaction of the adduct with the hydroxyl side chain of serine. On the other hand, the lack of adduct formation in G81D shows that a negative charge on the *re* side of FMN near the N5 position drastically alters the affinity for an adduct with a negatively charged ligand.

Redox Potential of FMN in wtMDH and the Gly81 Mutants. We measured the redox potentials of FMN in wtMDH and the mutants to examine whether changes at Gly81 altered the redox potential of FMN and if these changes could be correlated with the oxidase activities. Table 3 lists the potentials associated with the FMN_{ox}/FMN_{sq} redox couple, where FMN_{ox} is oxidized FMN and FMN_{sq} is the FMN semiquinone. wtMDH, MDH-GOX2, and the G81A mutants were observed to stabilize the anionic form of the FMN semiquinone, which has also been observed for other homologues in this protein family (data not shown) (*22*). wtMDH and MDH-GOX2 have identical redox potentials. On introducing the alanine mutation at Gly81 in both wtMDH and MDH-GOX2, the redox potential becomes ~30 mV more negative. For G81S, G81D, and G81V, the redox potential of the FMN_{ox}/FMN_{sq} couple is ~20, 30, and ~15 mV more negative compared to that of wtMDH.

DISCUSSION

The thermodynamically irreversible process of reoxidation of reduced flavin by molecular oxygen can be extremely fast or slow in flavoproteins. A case in point are the flavin-dependent mitochondrial acyl CoA dehydrogenase and peroxisomal acyl CoA oxidase families that both oxidize acyl CoAs to enoyl CoAs but react differently with oxygen. Flavodoxins form another flavoprotein family that reacts poorly with oxygen. Active-site features that lead to the suppression of activity with oxygen in certain flavoproteins are not yet clearly understood. This issue is especially interesting in the MDH family, where despite a high level of structural and sequence similarity, there is a large difference in reactivity toward oxygen between different subgroups. In the acyl CoA dehydrogenases, the enoyl-CoA product and the reduced FAD form a tight charge-transfer complex, which then transfers electrons to the electron-transferring flavoprotein. The oxidase activity is suppressed in the product-reduced enzyme complex; it is somewhat higher in the free reduced enzyme (*23*−*24*). Enzymes in the MDH family follow a ping-pong mechanism as demonstrated in studies of glycolate oxidase and MDH (*22*). The ping-pong mechanism in MDH holds true whether an artificial dye is used as the electron acceptor or oxygen (ref *18* and this paper). Therefore, it is clear that oxygen reactivity is significantly suppressed in the free reduced enzyme in MDH.

In the MDH family, the substrate-binding site as well as residues shown to be involved in the substrate oxidation reaction are located on the *si* face of the FMN (*8*). The residues on the *si* face are conserved in terms of both structure and sequence (*9*). However, structural comparisons reveal that there are subtle differences on the *re* face of the FMN. In particular, the localization of a four-residue peptide loop with respect to FMN is slightly different between the oxidase and the dehydrogenase subgroups; in the dehydro-

genases, the relative positions of FMN and the loop give rise to a more constrained geometry around the FMN N5 position.

A similar four-residue peptide loop plays an important role in flavodoxins. Structural studies have shown that a central peptide bond in this loop in flavodoxins is flipped after one-electron reduction of the FMN in flavodoxins; this change influences the redox potential of the FMN_{ox}/FMN_{sq} couple (*25*−*26*). Interestingly, extensive mutagenesis of the loop residues led to the conclusion that the side chains of the individual residues are not as important as the peptide backbone itself (*27*).

A recent high-resolution structural comparison of MDH-GOX2 in the oxidized and reduced states reveals that the locations of the residues on the *si* face remain relatively unchanged upon reduction (*28*). There is no peptide flip in the loop on the *re* face in the fully reduced structure; also, the loop does not undergo any major changes in localization. However, a structural water molecule, located in the vicinity of Gly81, is lost upon reduction of MDH-GOX2, resulting in a decreased flexibility of Gly81 in the reduced enzyme (*28*). We speculated that this decreased flexibility and the constraint imposed on the FMN N5 by the Gly81 loop may prevent facile reoxidation by oxygen. Interestingly, a sequence alignment reveals that all of the bacterial dehydrogenases in the MDH family have a strictly conserved glycine in this position, irrespective of the size of the substrate used by each enzyme.

Effect of the Gly81 Mutations on the FMN Environment. Though all of the Gly81 mutants were similar to wtMDH in terms of expression and stability, there were some differences in the FMN spectra and redox potential, indicating that the change at Gly81 affects the cofactor in subtle ways. The absorbance spectra of G81D and G81V were different from that of wtMDH. We expected that introducing an aspartate at residue 81 would be rather deleterious for the protein. This is indeed the case, given that G81D has very little activity. However, G81V shows a bigger change in the FMN absorbance spectrum and also extremely low activity. Presumably, introducing the large and branched side chain of valine in place of a hydrogen in the loop causes a major relocalization of the FMN.

Sulfite forms a covalent adduct with the electron-deficient oxidized FMN in the MDH family (*29*). The strength of the adduct depends on the electrophilicity of the flavin as well as interactions with various residues around the FMN. Because the dissociation constant of the adduct in G81A was similar to that in wtMDH, we can conclude that the overall environment around the FMN in G81A was relatively unchanged. However, because there was no adduct formation in G81D at all, the FMN N5 atom is probably quite electron-replete in G81D, and the low activity of G81D may result from the inability of the FMN to accept electrons from the substrate during its oxidation.

Redox potentials of the FMN_{ox}/FMN_{sq} couple in wtMDH are different from the Gly81 mutants, but they do not follow the same pattern as the overall catalytic activity or reactivity with oxygen. FMN in wtMDH has the same redox potential as the cytosolic MDH-GOX2, implying that removing the membrane-binding domain leaves the FMN unaffected. The redox potential is perturbed to the highest level when alanine replaces Gly81 in both wtMDH and MDH-GOX2, becoming 30 mV more negative. Aspartate causes a similar change, whereas the serine and valine replacements perturb the redox potential to a lesser extent. It is not clear why the alanine substitution results in such a large change in redox potential and electrophilicity of the FMN. It is possible that it results from a disruption of the hydrogen bond present between the FMN N5 and the Gly81 amide backbone (Figure 1).

Effect of Gly81 Mutations on Catalytic Activity and Substrate Specificity. Mutations at Gly81 have a substantial effect on the overall catalytic activity and the rate of the reductive reaction. G81A and G81S show 18- and ~130-fold lower k_{cat}, respectively; this is true for the rate of FMN reduction also. Substrate kinetic isotope effects are dramatically higher for G81A and G81S relative to that for wtMDH. In previous work, we have shown that wtMDH shows a distinct transient intermediate during the reaction with (*S*)-mandelate; this intermediate is a charge-transfer complex of the carbanion/enolate intermediate and oxidized FMN (*21*). The formation and breakdown of this intermediate, reflecting the formation and breakdown of the carbanion, have similar activation energies and are both rate-limiting for wtMDH. The first step is the isotope-sensitive step. As a consequence, wtMDH has only a partial $^{D}k_{cat}$ of ~2. Both G81A and G81S show a full $^{D}k_{cat}$ of >5. This clearly indicates that the rate-limiting step in the two mutants is now fully the α-carbon−hydrogen-bond-breaking step to generate the carbanion. Interestingly, the transient intermediate was also observed for G81A, though its extremely low extinction coefficient at its optimal wavelength precluded any meaningful analysis. However, it was evident that both the rates of formation and breakdown of the intermediate were slow in G81A compared to those in wtMDH. Together with the observation that the redox potential of the $FMN_{ox} \rightarrow FMN_{sq}$ couple is 30 mV more negative in G81A, these results show that the mutation reduces the electrophilicity of the FMN. This, in turn, causes a destabilization of the carbanion because the electrophilic oxidized FMN may be one of the factors that stabilizes the carbanion in this protein family. The decreased electrophilicity also causes a decrease in the rate of electron transfer to the FMN, concomitant with the breakdown of the carbanion intermediate.

When our results are compared with those obtained with the corresponding mutations in other members of the MDH family, it is evident that the homologous residue has different effects on the substrate oxidation/FMN reduction half-reaction for the different enzymes. Catalytic activity increased with larger side-chain substrates for the alanine to glycine modification in lactate oxidase (*14*). The alanine to glycine modification in flavocytochrome b_2 resulted in a slight decrease in k_{red} and a modest decrease in substrate affinity, while the glycine to alanine or serine mutations in lactate monooxygenase had little effect on the first half-reaction (*13*, *15*−*16*). However, in MDH, there was a significant *decrease* in catalytic activity and the rate of the first half-reaction for the G81A and G81S mutants. Though the affinity for (*S*)-mandelate was not greatly altered, the specificity constant improved for smaller substrates. These observations suggest that changing Gly81 probably has a more significant effect on the FMN environment in MDH and perhaps the bacterial dehydrogenase subgroup, relative to the other two subgroups of this protein family.

Effect of Gly81 Mutations on the Activity with Oxygen. The most interesting finding in our studies of the mutation at Gly81 is that the affinity for oxygen improved ~10-fold when glycine was replaced by alanine. The rate of the oxidative reaction by oxygen also improved 2−3-fold. This is the first instance where a mutation was observed to increase the overall activity with oxygen in the MDH family. The residue corresponding to Gly81 and probably the loop containing this residue does seem to play a role in controlling oxygen affinity and/or activity in some members of the MDH family. In MDH and lactate monooxygenase, the glycine to alanine mutation resulted in opposite effects; the activity with oxygen increased modestly in MDH and was drastically reduced in lactate monooxygenase. However, in lactate oxidase, the activity was relatively unchanged.

Structural data of the G81A mutant (studies in progress) may explain why the affinity for oxygen improves in G81A and G81S. It is likely that a larger side chain at residue 81 causes the loop to move away from FMN, creating more space for the oxygen molecule to bind, and an increased affinity. The modest improvement in the rate of the reaction with oxygen for G81A is also likely to be due to a more optimal orientation of the bound oxygen molecule, such that it can form the FMN-4a hydroperoxide intermediate. Alternatively, it is possible that the change in the hydrogen-bonding network with structural water molecules that we observed in the structure of reduced MDH-GOX2 is somewhat altered in reduced G81A, resulting in a different degree of desolvation of the active site. It has been proposed that oxidase activity may be controlled in part by solvation, because the redox potential of the $O_2 \leftrightarrow O_2^-$ couple is strongly solvent-dependent (*30*). Surprisingly, the activities with oxygen for the different Gly81 mutants were not correlated with the redox potential of the $FMN_{ox} \rightarrow FMN_{sq}$ couple, implying that redox potential differences cannot explain the low reactivity of the dehydrogenases with oxygen. Further investigation of the relative positions of FMN and the loop in MDH and their effect on the activity with oxygen will help to clarify whether steric and/or solvation effects are more important in regulating oxygen reactivity.

Conclusions. Gly81, part of a loop adjacent to the FMN in MDH, plays an important role in both the first reductive half-reaction and in the second oxidative half-reaction with oxygen. Residues with larger side chains result in a decrease in the overall activity and in the rate of the first half-reaction. This decrease in the rate of the reductive half-reaction is likely due to the decreased electrophilicity of the FMN. Though the mutations did not alter the affinity for (*S*)-mandelate, the affinity for smaller substrates increased in G81A compared to wtMDH. The membrane-binding segment of wtMDH does not suppress the reaction with oxygen, because a soluble mutant MDH-GOX2, in which this segment was absent, had an even lower activity with oxygen compared to wtMDH. Reactivity with oxygen appears to be controlled, at least in part, by the constraints imposed by the Gly81-containing loop, as observed by the G81A mutation in both wtMDH and MDH-GOX2. The rate of the oxidative half-reaction with oxygen increased for the G81A mutants; this was primarily a result of an increased affinity for oxygen. This may be due to a breaking of a hydrogen bond between the FMN and the Gly81 amide as well as the repositioning of the FMN and the loop.

REFERENCES

1. Tsou, A. Y., Ransom, S. C., Gerlt, J. A., Buechter, D. D., Babbitt, P. C., and Kenyon, G. L. (1990) Mandelate pathway of *Pseudomonas putida*: Sequence relationships involving mandelate racemase, (*S*)-mandelate dehydrogenase, and benzoylformate decarboxylase and expression of benzoylformate decarboxylase in *Escherichia coli*, *Biochemistry 29*, 9856−9862.
2. Diêp Le, K. H., and Lederer, F. (1991) Amino acid sequence of long chain α-hydroxy acid oxidase from rat kidney, a member of the family of FMN-dependent α-hydroxy acid-oxidizing enzymes, *J. Biol. Chem. 266*, 20877−20881.
3. Reid, G. A., White, S., Black, M. T., Lederer, F., Mathews, F. S., and Chapman, S. K. (1988) Probing the active site of flavocytochrome b_2 by site-directed mutagenesis, *Eur. J. Biochem. 178*, 329−333.
4. Lockridge, O., Massey, V., and Sullivan, P. A. (1972) Mechanism of action of the flavoenzyme lactate oxidase, *J. Biol. Chem. 247*, 8097−8106.
5. Matsushita, K., and Kaback, H. R. (1986) D-Lactate oxidation and generation of the proton electrochemical gradient in membrane vesicles from *Escherichia coli* GR19N and in proteoliposomes reconstituted with purified D-lactate dehydrogenase and cytochrome *o* oxidase, *Biochemistry 25*, 2321−2327.
6. Dong, J. M., Taylor, J. S., Latour, D. J., Iuchi, S., and Lin, E. C. C. (1993) Three overlapping lct genes involved in L-lactate utilization by *Escherichia coli*, *J. Bacteriol. 175*, 6671−6678.
7. Lindqvist, Y. (1989) Refined structure of spinach glycolate oxidase at 2 Å resolution, *J. Mol. Biol. 209*, 151−166.
8. Xia, Z., and Mathews, F. S. (1990) Molecular structure of flavocytochrome b_2 at 2.4 Å resolution, *J. Mol. Biol. 212*, 837−863.
9. Lindqvist, Y., Brändén, C.-I., Mathews, F. S., and Lederer, F. (1991) Spinach glycolate oxidase and yeast flavocytochrome b_2 are structurally homologous and evolutionarily related enzymes with distinctly different function and flavin mononucleotide binding, *J. Biol. Chem. 266*, 3198−3207.
10. Sukumar, N., Xu, Y., Gatti, D. L., Mitra B., and Mathews, F. S. (2001) Structure of an active soluble mutant of the membrane-associated (*S*)-mandelate dehydrogenase, *Biochemistry 40*, 9870−9878.
11. Massey, V. (1994) Activation of molecular oxygen by flavins and flavoproteins, *J. Biol. Chem. 269*, 22459−22462.
12. Xu, Y., and Mitra, B. (1999) A highly active, soluble mutant of the membrane-associated (*S*)-mandelate dehydrogenase from *Pseudomonas putida*, *Biochemistry 38*, 12367−12376.
13. Daff, S., Manson, F. D., Reid, G. A., and Chapman, S. K. (1994) Strategic manipulation of the substrate specificity of *Saccharomyces cerevisiae* flavocytochrome b_2, *Biochem. J.* 301, 829−834.
14. Yorita, K., Aki, K., Ohkuma-Soyejima, T., Kokubo, T., Misaki, H., and Massey, V. (1996) Conversion of L-lactate oxidase to a long chain α-hydroxyacid oxidase by site-directed mutagenesis of alanine 95 to glycine, *J. Biol. Chem. 271*, 28300−28305.
15. Sun, W., Williams, C. H., and Massey, V. (1996) Site-directed mutagenesis of glycine 99 to alanine in L-lactate monooxygenase from *Mycobacterium smegmatis*, *J. Biol. Chem. 271*, 17226−17233.
16. Sun, W., Williams, C. H., and Massey, V. (1997) The role of glycine 99 in L-lactate monooxygenase from *Mycobacterium smegmatis*, *J. Biol. Chem. 272*, 27065−27076.
17. Landro, J. A., Kallarakal, A. T., Ransom, S. C., Gerlt, J. A., Kozarich, J. W., Neidhart, D. J., and Kenyon, G. L. (1991) Mechanism of the reaction catalyzed by mandelate racemase. 3. Asymmetry in reactions catalyzed by the H297N mutant, *Biochemistry 30*, 9274−9281.
18. Lehoux, I. E., and Mitra, B. (1999) (*S*)-Mandelate dehydrogenase from *Pseudomonas putida*: Mechanistic studies with alternate substrates and pH and kinetic isotope effects, *Biochemistry 38*, 5836−5848.
19. Massey, V. (1991) A simple method for the determination of redox potentials, in *Flavins and Flavoproteins*, (Curti, B., et al., Eds.) pp 59−66, Walter de Gruyter, New York.
20. Stankovich, M. T., Schopfer, L. M., and Massey, V. (1978) Determination of glucose oxidase oxidation−reduction potentials and the oxygen reactivity of fully reduced and semiquinoid forms, *J. Biol. Chem. 253*, 4971−4979.
21. Dewanti, A. R., and Mitra, B. (2003) A transient intermediate in the reaction catalyzed by (*S*)-mandelate dehydrogenase from *Pseudomonas putida*, *Biochemistry 42*, 12893−12901.

22. Macheroux, P., Massey, V., Thiele, D. J., and Volokita, M. (1991) Expression of spinach glycolate oxidase in *Saccharomyces cerevisiae*: Purification and characterization, *Biochemistry 30*, 4612−4619.
23. DuPlessis, E. R., Pellett, J., Stankovich, M. T., and Thorpe, C. (1998) Oxidase activity of the acyl-CoA dehydrogenases, *Biochemistry 37*, 10469−10477.
24. Wang, R., and Thorpe, C. (1991) Reactivity of medium-chain acyl-CoA dehydrogenase toward molecular oxygen, *Biochemistry 30*, 7895−7901.
25. Romero, A., Caldeira, J., Legall, J., Moura, I., Moura, J. J., and Romao, M. J. (1996) Crystal structure of flavodoxin from *Desulfovibrio desulfuricans* ATCC 27774 in two oxidation states, *Eur. J. Biochem. 239*, 190−196.
26. Ludwig, M. L., Pattridge, K. A., Metzger, A. L., Dixon, M. M., Eren, M., Feng, Y., and Swenson, R. P. (1997) Control of oxidation−reduction potentials in flavodoxin from *Clostridium beijerinckii*: The role of conformation changes, *Biochemistry 36*, 1259−1280.
27. Kasim, M., and Swenson, R. P. (2001) Alanine-scanning of the 50's loop in the *Clostridium beijerinckii* flavodoxin: Evaluation of additivity and the importance of interactions provided by the main chain in the modulation of the oxidation−reduction potentials, *Biochemistry 40*, 13548−13555.
28. Sukumar, N., Dewanti, A. R., Mitra, B., and Mathew, F. S. (2004) High-resolution structures of an oxidized and reduced flavoprotein: The water switch in a soluble form of (*S*)-mandelate dehydrogenase, *J. Biol. Chem. 279*, 3749−3757.
29. Muller, F., and Massey, V. (1969) Flavin−sulfite complexes and their structures, *J. Biol. Chem. 244*, 4007−4016.
30. Sawyer, D. T., and Nanni, E. J. (1981) in *Oxygen and Oxy-Radicals in Chemistry and Biology*, (Sawyer, D. T., and Nanni, E. J., Eds.) pp 15−44, Academic Press, New York.
31. Volokita, M., and Somerville, C. R. (1987) The primary structure of spinach glycolate oxidase deduced from the DNA sequence of a cDNA clone, *J. Biol. Chem. 262*, 15825−15828.
32. Jones, J. M., Morrell, J. C., and Gould, S. (2000) Identification and characterization of HAOX1, HAOX2, and HAOX3, three human peroxisomal 2-hydroxy acid oxidases, *J. Biol. Chem. 275*, 12590−12597.
33. Maeda-Yorita, K., Aki, K., Sagai, H., Misaki, H., and Massey, V. (1995) L-Lactate oxidase and L-lactate monooxygenase: Mechanistic variations on a common structural theme, *Biochimie 77*, 631−642.
34. Guiard, B. (1985) Structure, expression, and regulation of a nuclear gene encoding a mitochondrial protein: The yeast L(+)-lactate cytochrome *c* oxidoreductase (cytochrome b_2), *EMBO J. 4*, 3265−3272.
35. Risler, Y., Tegoni, M., and Gervais, M. (1989) Nucleotide sequence of the *Hansenula anomala* gene encoding flavocytochrome b_2 (L-lactate:cytochrome *c* oxidoreductase), *Nucleic Acids Res. 17*, 8381.
36. Illias, R. M., Sinclair, R., Robertson, D., Neu, A., Chapman, S. K., and Reid, G. A. (1998) L-Mandelate dehydrogenase from *Rhodotorula graminis*: Cloning, sequencing, and kinetic characterization of the recombinant enzyme and its independently expressed flavin domain, *Biochem. J. 333*, 107−115.

BI049005P